Bulletin of Earthquake Engineering (2025) 23:1017–1052
https://doi.org/10.1007/s10518-024-01941-w

ORIGINAL ARTICLE

Seismic performance of retrofitted and non-retrofitted RC school buildings after the February 6th, 2023, Kahramanmaraş earthquakes

Taha Yasin Altıok[1] · **Mehmet Şevik**[1] · **Ali Demir**[1]

Received: 19 October 2023 / Accepted: 18 May 2024 / Published online: 1 August 2024
© The Author(s) 2024

Abstract
On February 6, 2023, two significant earthquakes struck Pazarcık and Elbistan/Kahramanmaraş with magnitudes of 7.7 and 7.6, respectively. These earthquakes are considered the most devastating disaster in Turkey in the last century. According to official records, these earthquakes affected 11 provinces, resulting in the loss of more than 50,000 lives. Additionally, numerous buildings collapsed or became unusable due to the impact of the earthquakes and the schools constitute an important part of these structures. The schools are important facilities that need to be functional and safe following an earthquake. This study contains both post-earthquake field observations and numerical studies for the retrofitted and non-retrofitted schools. It investigates the retrofitted and non-retrofitted conditions of a total of 7 blocks, which consist of 4 different schools located in Kahramanmaraş. It is observed that the retrofitted school buildings weren't damaged after these earthquakes. The numerical models underwent nonlinear time history analyses using the ETABS program. The ground accelerations used in the analyses were obtained from the nearest station to the school buildings. The analyses yielded several results, including the natural periods, story displacements, story drifts, and seismic energy inputs of the structures. These results were then compared with the field observations to assess their accuracy and validity. With the retrofit application, story displacements, the interstory drifts and seismic energy input have decreased. Both field studies and numerical analyses have shown that even school buildings with insufficient material and engineering services can become resistant to major earthquakes with an appropriate retrofit method.

Keywords Kahramanmaraş earthquakes · Structural behavior · Non-linear analysis · Time-history · Performance-based design · Seismic retrofitting

✉ Taha Yasin Altıok
taha.altiok@cbu.edu.tr

Mehmet Şevik
ssevik.mehmet@gmail.com

Ali Demir
ali.demir@cbu.edu.tr

[1] Department of Civil Engineering, Manisa Celal Bayar University, P.O.45125, Manisa, Turkey

1 Introduction

Buildings located in high seismicity regions can cause serious damage in large earthquakes and threaten life and property safety. Many buildings were damaged and collapsed in earthquakes in the past (Menoni 2001; Yakut et al. 2005; Martinelli et al. 2008; Miura et al. 2008; Gunes 2015; Damcı et al. 2015; Sharma et al. 2016). The common features of the structures damaged in the earthquakes in Turkey are low quality concrete, insufficient development lengths, insufficient stirrup use, faulty stirrup hook angle, and structural defects such as strong beam and weak column problems (Yakut et al. 2005; Kucukgoncu and Altun 2020). Most of these structures, which are not built based on modern codes, do not have sufficient lateral load-bearing capacity, lateral rigidity, energy dissipation capacity and ductility (Sezen et al. 2003; Canbay et al. 2003; Erdem et al. 2006; Belleri et al. 2015; Ahmad et al. 2017; Rizwan et al. 2019). As a result of this situation, these structures under dynamic effect are exposed to displacement demands that cannot be adequately met. The reconstruction of structures with insufficient lateral rigidity can be quite costly. For this reason, various retrofitting methods are applied to improve the earthquake behaviour of buildings and to prevent loss of life and property (Elnashai and Pinho 1998; Bal et al. 2011; Calvi 2013). Retrofitting is basically divided into two categories: global retrofitting and local retrofitting. In general retrofitting methods, the structure is usually retrofitted to limit lateral displacements to compensate for the condition of low ductility (Sonuvar et al. 2004). Local retrofitting, on the other hand, can be summarized as the improvement of the structural load-bearing element by eliminating the deficiency. However, in this method, if the number of elements increases, there may be greater costs compared to the global retrofitting. The most commonly used technique in the global retrofitting method is reinforced concrete (RC) shear wall retrofit. This method greatly increases the lateral load capacity and rigidity (Jirsa and Kreger 1989; Altin et al. 1992; Albanesi et al. 2008). It gives satisfactory results even when applied in damaged buildings (Canbay et al. 2003; Sonuvar et al. 2004).

Schools constitute an important part of the buildings damaged and collapsed in earthquakes. School buildings are among the basic elements that shape our society from a social point of view. Schools are buildings that require post-earthquake usage and are among the structures where people stay for a long time and intensely. The safe evacuation of students from these buildings after an earthquake, and subsequently ensuring the continuity of education and post-earthquake gathering center activities, is contingent upon the performance of these structures. Many of Turkey's school buildings were built before modern seismic codes between generally 1970–1995 years.

Several countries, including the United States, Canada, and Mexico in the Americas, and European countries like Turkey and Italy, as well as Asian countries such as Japan, have allocated various funds to contribute to the renovation and retrofitting of school structures located in seismically hazardous regions (Di Ludovico et al. 2019). There are various studies in the literature about earthquake resistant structures and retrofit works. Today, steel and RC jacketing (Erange et al. 2023; Hung et al. 2023), shear wall additions, retrofitting with steel bracing (Souri and Mofid 2023), fiber-reinforced polymer applications (El-Sokkary 2023), and energy dissipation systems (Santos et al. 2019) are commonly used to protect the superstructure against to earthquakes. Samadian et al. (2019), in their studies on a retrofitted school structure, has determined that retrofitting has a significant impact on improving seismic resilience and reducing structural vulnerability. Rodrigues et al. (2018) identified in their nonlinear analyses on a typical school building that retrofitting methods

reduce seismic vulnerability. Ahmad et al. (2019) the haunch retrofitting technique has been used to enhance the seismic resistance of RC frame structures by retrofitting beam-column connections and preventing shear hinging, and appropriate strategies for risk reduction have been identified based on conducted tests and analyses. Ahmad and Masoudi (2020) presents a seismic retrofit design of RC frames using internal eccentric steel braces (ESBs) with a simplified static-force-based procedure, aiming to reduce elastic base shear and demonstrating the effectiveness of the ESB retrofit technique. Haghpanah et al. (2017) conducted a study on a four-story school building, examining the structural effects of three different retrofitting methods: base isolator, concrete, and steel jacketing. The research findings revealed that, despite the success of jacketing in limiting floor displacements, they were unable to achieve the desired performance level. Conversely, it was determined that the base isolator provided positive results in terms of economic feasibility, sustainability, and safety. Carofilis et al. (2020) investigated different retrofitting techniques for three typical school structures in the Italian school building stock, which are RC, precast concrete (PC), and unreinforced masonry (URM). Fiber reinforced polymer (FRP) and steel bracing were evaluated for RC structures, steel bracing and viscous dampers for PC structures, and FRP and viscous dampers for URM structures. Almeida et al. (2017) the retrofitting of a 3-story school building located in a highly seismic region of Portugal using Buckling Restrained Braces (BRB) elements has been evaluated. It has been observed that BRB elements are an effective way to enhance the performance of structures that do not comply with current seismic codes. Meglio et al. (2023) conducted a numerical analysis on the retrofitting of a RC school structure using a lightweight metal external frame method without affecting its use. It was determined that the method would be efficient in school structures with a regular geometric plan.

Markou (2021) the study evaluates FRP and shear wall retrofitting in terms of cost-effectiveness. The results indicate that shear walls are the most effective retrofitting method in terms of both strength and energy absorption. Pall (2004) the use of Pall friction dampers has been shown to provide a practical, economical, and effective approach. The savings achieved in some significant structures constructed with friction dampers have been discussed. Dumaru et al. (2019) in the study, cost-effectiveness analyses of different retrofitting techniques were evaluated, and it was found that buildings retrofitted with RC shear walls are the most economically viable, followed by steel bracing and jacketing, respectively.

This study evaluates the post-earthquake observations in the Kahramanmaraş region and the seismic performance of both retrofitted and non-retrofitted school buildings. The potential damage that would have occurred in non-retrofitted school buildings if they were not retrofitted has also been assessed. The nearest stations to the school buildings were determined, and nonlinear time history analyses were performed using the recorded ground motion data from these stations. The story displacements, story drifts, seismic energy inputs, and damage states of the building elements were determined.

1.1 Earthquake history of Turkey

Turkey is a country that is frequently exposed to earthquakes due to its geological location. The main seismic belts in Turkey are the Northern Anatolian Seismic Belt, the Southeastern Anatolian Seismic Belt and the Western Anatolian Seismic Belt. In the last 50 years, Turkey has experienced 1975 Lice, 1976 Çaldıran, 1983 Erzurum, 1992 Erzincan, 1998 Adana-Ceyhan, 1999 Gölcük, 1999 Düzce, 2003 Bingöl, 2011 Van, 2020 Elazığ and Seferihisar

and lastly 2023 Kahramanmaraş earthquakes. Failure to comply with the regulations, uncontrolled manufacturing, not using ready-mixed concrete, and unribbed reinforcement resulted in loss of life and property during earthquakes. We see similar scenes in every earthquake from past to present. Soft floor effect, torsional irregularity, adherence and development length problems, lack of shear wall use, soil problems, etc. problems are encountered in most earthquakes. Bayraktar et al. (2013) After the earthquakes in Van with magnitudes of 7.2 and 5.6, occurring on October 23 and November 9, 2011, respectively, field observations were conducted, and structural damages in RC structures were examined in detail. Oyguc (2016) discussed the performance and field observations of two school buildings, one damaged and the other undamaged, after the Van earthquakes that occurred on October 23 and November 9, 2011. Altunişik et al. (2021) The examination of damages and collapses in structures resulting from the 6.9 magnitude earthquake and tsunami that occurred off the coast of Samos Island in October 2020 has been conducted. Demir et al. (2021) In the earthquake that occurred in Elazığ in 2020, the performance of RC structures was evaluated by examining ground motion records. The observed designs and implementations were assessed, and the obtained results were compared according to the Turkish Earthquake Code. Dogan et al. (2021) After the 6.8 magnitude earthquake that occurred in Elazığ on January 24, 2020, the damages encountered in the RC structures in the region were examined and interpreted according to the Turkish Earthquake Code. Demirel et al. (2022) Following the 6.9 magnitude earthquake off the Samos Island of Greece on October 30, 2020, which also affected Izmir, the structural performance of 140 RC buildings with 7 to 12 story was examined in detail as a result of field observation. Mertol et al. (2023) the earthquake acceleration records of the earthquakes that occurred in Pazarcık and Elbistan in February 2023 have been examined. Additionally, the findings, observations and evaluations of the technical team sent to the region regarding the destroyed and damaged buildings have been presented. Altunişik et al. (2023) Pazarcık and Elbistan earthquakes in February 2023 have been examined. The field observations in the earthquake-prone area were examined, along with the faults in the design and construction stages.

1.2 Site survey of post-disaster schools in Kahramanmaraş earthquakes

A major earthquake and hundreds of aftershocks occurred in the Pazarcık and Elbistan districts of Kahramanmaraş on February 6, 2023, resulting in numerous deaths and injuries. These earthquakes are the largest earthquakes to occur within the borders of Turkey in the last century. The first earthquake occurred at 4:17 a.m. in Pazarcık with a magnitude of 7.7. Some structures in the Pazarcık earthquake, despite not collapsing, have suffered damage and undergone plastic deformation. In the second earthquake that took place at 1:24 p.m. in Elbistan with a magnitude of 7.6, those buildings either collapsed or sustained severe damage. As far as is known, while more than 50,000 people lost their lives, the survivors have been exposed to the psychological effects of the earthquake.

This study primarily focuses on school buildings, where individuals spend extended periods of time. Analytical investigations complementing field observations have been conducted regarding the causes of damage and collapses in both retrofitted and non-retrofitted schools within the earthquake-affected region. Destructive earthquakes have had a notable impact on educational institutions. Following the earthquake, educational facilities were classified into four damage levels (Table 1). The damage status of 3440 educational facilities in the region was thoroughly investigated, revealing that 2533 of them had suffered

Table 1 Explaining the damage levels of educational structures (SBB 2023)

Damage level	Description
Slight damage	The buildings where the load-bearing system has almost no damage, but non-load-bearing walls have damage such as cracks, paint/coating flaking, etc
Moderate damage	The buildings that require retrofitting due to the extent of damage they have suffered. Such buildings cannot be used without retrofitting
Heavy damage	Buildings that have been damaged to the extent that repair is not possible, and reuse is not feasible are classified as heavily damaged
Destruction	Some or all stories have collapsed, tilted, shifted, etc. buildings that have been damaged to a large extent and threaten the safety of life and property at any time

slight damage, 331 had moderate damage, 504 had heavy damage, and 72 were completely destroyed. Figure 1 provides the percentage distribution of educational facilities according to the damage levels given in Table 1. According to Fig. 1, 73.6% of educational facilities have suffered slight damage, 14.7% heavy damage, 9.6% moderate damage, and 2.1% resulted in destruction. The prevalent damage in schools typically comprises inadequate adherence and development length, insufficient spacing of stirrup bars and a 90° hook, deficiencies in columns/shear walls, the presence of soft stories, concrete quality, corrosion, structural system irregularities, and short columns. This section delves into some of the specific structural damage causes in detail.

1.3 The general structural damages observed after the earthquake.

Each damage occurring in the load-bearing system should be meticulously investigated. The occurrence of damage in these elements indicates a decrease in the element's strength. Earthquake-induced damages to the load-bearing system can generally be categorized under two headings: 'Damages resulting from design mistakes' and 'Damages resulting from implementation mistakes' (Atmaca et al. 2020). Examples of design mistakes include strong beam-weak column damages, short column damages, soft-story damages, damages

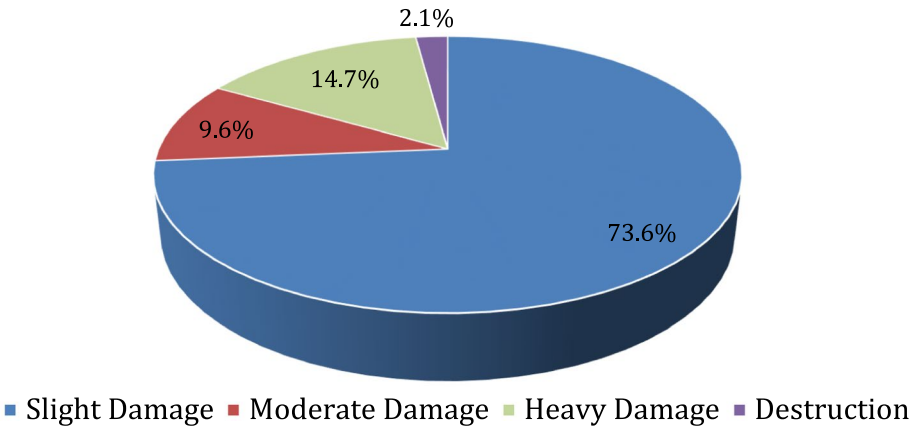

Fig. 1 Damage levels of educational facilities earthquake region

due to pounding and insufficient joint clearance, corner column damages, short and unconfined splices (adhesion problems), damages due to inadequate stirrups, column-beam junction area damages, shear damages in shear walls and columns, and beam damages. Examples of damages resulting from implementation mistakes include inadequate concrete strength and damages due to the use of inappropriate aggregates, damages due to reinforcement corrosion, damages resulting from incorrect placement of reinforcements, damages due to incorrect hook angles of stirrups, and damages resulting from labor mistakes.

Engineering service may characterize deficiencies in design field applications and their inspection. Many damaged and collapsed structures in the earthquake region do not meet modern earthquake code conditions. In addition, there are deficiencies in the application phase of projects prepared in accordance with the regulations. The emergence of the concept of building inspection, which is the mechanism that controls all of these, in Turkey in the early 2000s shows the lack of engineering services for buildings.

1.3.1 Damages arising from issues in the load-bearing system

The loads affecting the structure must be safely transferred to the ground in the shortest path possible. In Türkiye Building Earthquake Code (TBEC-2018), it has been emphasized that irregularities in the plan and vertical irregularities should be avoided in the arrangement of building structural systems. Additionally, it is stated that structural systems should exhibit basic, regular, symmetrical, sufficient strength, sufficient rigidity, sufficient ductility, and excessive connectivity (hyperstatic behavior). The regularity and continuity of vertical and horizontal load-bearing elements ensure that structures are less affected by earthquake forces. In the context of earthquake zone inspections, it has been observed that schools typically have rectangular-shaped floor plans, continuous beams along the axis, and columns placed in both directions. Therefore, schools have been among the structures with the least damage and collapse.

1.3.2 Strong beam–weak column damages

The strong column weak beam principle is crucial for structures to exhibit ductile behavior. According to this principle, earthquake energy is dissipated in ductile beams. In TBEC-2018, the load-carrying capacity moments of columns in the joint region should be at least 20% greater than the sum of the load-carrying capacity moments of the beams connected to the nodal point (Fig. 2). In many existing structures in our country, contrary to this principle, strong beam weak column mistakes are observed. This situation leads to the formation of plastic hinges in column elements before beams. Hinges formed in vertical load-bearing systems result in partial or total collapse of structures. An example of a school that has suffered from the strong beam weak column problem in an earthquake-prone area is shown in Fig. 3.

1.3.3 Short column damage

The effective lengths of columns are often reduced, usually due to architectural considerations. During an earthquake, as the column shortens, its lateral displacement rigidity increases, exposing it to more shear force than anticipated in the design phase. In this situation, severe shear damages occur in the column, which can lead to brittle fractures

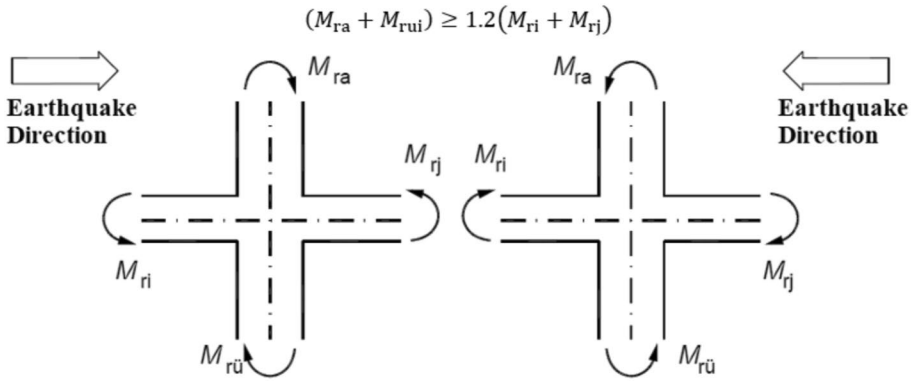

Fig. 2 The strong column–weak beam principle



Fig. 3 Collapse of a story due to strong beam–weak column damage

(Fig. 4). In cases where the formation of short columns cannot be prevented, TBEC-2018 increases the shear force. Additionally, it mandates the application of defined minimum stirrup bar and placement conditions for the confinement regions along the entire length of the columns.



Fig. 4 Short column damage due to ribbon window

1.3.4 Soft story damage

TBEC-2018 defines the condition of soft story irregularity as the ratio of the interstory drift occurring in any story to the story immediately above or below it being greater than 2. Structures exhibiting this irregularity are not allowed to use equivalent earthquake load analysis. Especially in the ground stories of structures, infill walls are significantly reduced compared to upper stories. Additionally, the heights of ground stories can be greater than other stories. This situation diminishes the lateral displacement rigidity contributed by walls and reduces the lateral displacement rigidity of the story due to an increase in the effective length of the column. During an earthquake, these stories with low horizontal displacement rigidity undergo more lateral displacements compared to other stories. Due to different lateral displacements, the continuity of the vertical load-bearing system between stories is disrupted, leading to damages and even collapses in structures (Fig. 5).



Fig. 5 Soft story damage due to lack of infill wall

1.3.5 Inadequate adherence, development length and lap splice length

For a RC structural element to behave as required, it is imperative that the reinforcement is well anchored to the concrete. The required development length for achieving complete adherence depends on the positioning of the reinforcement bars in concrete. The development length is the minimum embedment depth that can provide anchorage strength equal to the yield strength of the reinforcement bar. In any RC section, the reinforcement must have sufficient development length in both directions to safely carry the anticipated tensile or compressive stresses (Fig. 6.). According to TBEC-2018, In the case of straight embedding, the development length is calculated as given in Eq. 1 for ribbed reinforcements. For unribbed reinforcements, this length is multiplied by 2. The development length varies in situations such as changes in the inclination of the reinforcement within the concrete, variations in section dimensions between floors, and other factors.

$$\ell_b = \left(0{,}12\frac{f_{yd}}{f_{ctd}}\phi\right) \geq 20\phi \tag{1}$$

Inadequate adherence, development length and lap splice length problems, which are very important problems in terms of structural integrity, are frequently encountered in the earthquake region. Lap splice and development lengths play a crucial role in ensuring continuity between floors. Adequate lap splice and development length increase the adherence strength between concrete and reinforcement, ensuring the yield of reinforcement without collapse. This behavior is among the essential conditions of ductile design. During the earthquake, inadequate lap splice and development lengths have been observed to lead to inadequate adherence, resulting in the debonding of reinforcements and structural damage (Fig. 7).

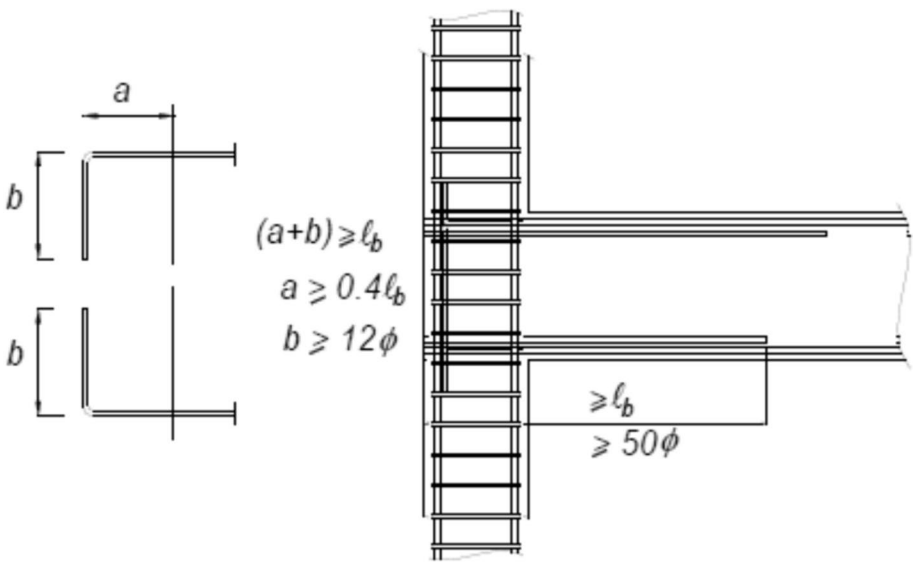

Fig. 6 Details of development length according to TBEC-2018



Fig. 7 Lack of adherence and development length problems

1.3.6 Inadequate stirrup bar

To reduce the shear force damage on structural elements during an earthquake, the number and diameter of stirrups play a significant role. Stirrup bars should undergo densification, particularly in regions where plastic behavior is expected, i.e. at both ends of structural elements. TBEC-2018 provides detailed information about stirrup spacings and confinement zone lengths for structural system elements (Fig. 8). According to the regulations, 135° bent hooks must be present at both ends of the stirrups. This was not taken into consideration in many buildings that were damaged or collapsed in the earthquake region. Many structures have been encountered where the stirrup spacing is around 200–250 mm. In addition, one of the important shortcomings is that the hook angles are applied at 90° instead of 135°. The damages caused by insufficiency of stirrups and hook angles are provided in Fig. 9.

1.3.7 Inadequate concrete grade

Concrete strength is a parameter that directly influences the behavior of the structural system. According to TBEC-2018, the use of concrete with compressive strength lower than 25 MPa is not allowed in RC buildings. Although Turkey ranks first among the European countries in ready-mixed concrete production today, the history of ready-mixed concrete has a very short history in Turkey. Before ready-mixed concrete became widespread and mandatory, concrete production was generally carried out directly on construction sites. Most of this production took place without engineering

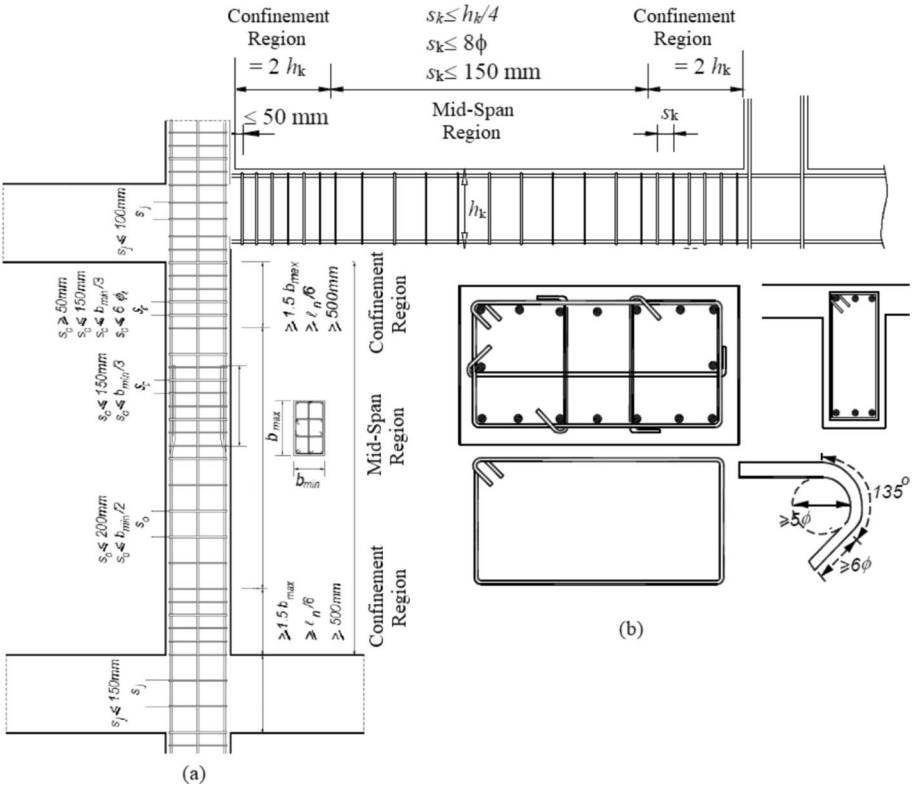

Fig. 8 Placement and details of stirrups according to TBEC-2018

supervision. The limited use of ready-mixed concrete technology in many buildings in Turkey before 2000 resulted in certain issues. Especially in earthquake regions, a significant part of the building stock before 2000 was seriously damaged or completely destroyed due to inadequate concrete quality (Fig. 10).

1.3.8 Gable wall damage

The walls on the two inclined sides of the roof are typically associated with the triangular shape of the roof. These walls can collapse if not supported by horizontal and vertical bond beams (Fig. 11). To prevent damage to gable walls, TBEC-2018 requires the installation of vertical and diagonal ties when the height of the roof diaphragm supported by a horizontal bracing wall exceeds 0.80 m (Fig. 12).

1.3.9 Inadequate construction joint damages

In the case of inadequate joints between adjacent regular structures with different periods, a pounding effect occurs during an earthquake due to the collision of the structures with each other. The pounding effect can result in significant damage, especially in the vertical



Fig. 9 Inadequate stirrup spacing and 90° hook angles



Fig. 10 Damages caused by inadequate concrete strength and inappropriate aggregate use

load-bearing systems of the structures. These damages can lead to partial or total collapses (Fig. 13). TBEC-2018 introduces certain rules regarding joint clearances between adjacent regular-shaped structures. According to the regulation articles, the minimum joint

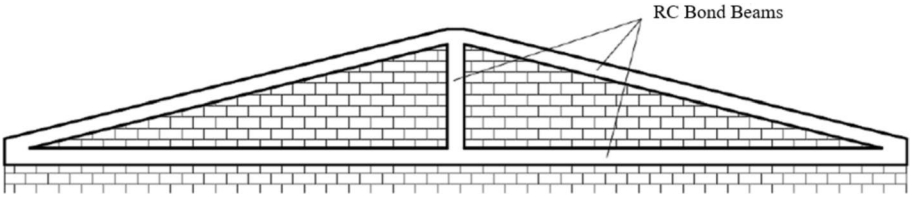

Fig. 11 Gable wall detail with a height greater than 0.80 m



Fig. 12 Gable wall damages seen in school buildings

clearance is at least 30 mm up to a height of 6 m, and beyond 6 m, an additional 10 mm will be added for every 3 m of height. This value should not be less than the product of the "a" coefficient, obtained by multiplying the square root of the sum of squares of displacements achieved in adjacent blocks or buildings for each floor, and 0.5× (R/I) in case of different floor levels of adjacent structures, or 0.25× (R/I) if the floor levels are the same. Here, R refers to the load-bearing system behavior coefficient and I refers to the building importance coefficient. Additionally, joints should be designed to enable blocks to operate independently in all directions during an earthquake.



Fig. 13 Pounding damages in school structures

2 Seismic performance of school structures following the Kahramanmaras earthquake

2.1 RC school structures

The project of some retrofitted school structures was obtained. Nonlinear time history analyses were conducted using the ETABS program. The analyses were performed under the seismic accelerations of the nearest station. The results obtained were presented comparatively. In this context, some information about the examined school structures is given in Table 2. The 3D numerical models of these school structures and retrofitted formwork plans with shear walls are given in Fig. 14. The elements shown in yellow colour in the formwork plans represent the retrofitting shear walls. The yield strength of StIII type reinforcement is considered as 420 MPa, while the yield strength of STI type reinforcement is considered as 220 MPa for the existing reinforcement strength. The soil properties ZD refers to the ground containing medium-firm and dense layers of sand, gravel or very solid clay, ZC refers to very dense sand, gravel and hard clay layers or decomposed, very cracked weak rocks, Z4 refers to loose sand, soft clay, silty clay soil.

2.2 Nonlinear time history analysis

2.2.1 Earthquake acceleration records

In this study, nonlinear time history analyses of retrofitted school buildings were performed according to the TBEC-2018 conditions. Four retrofitted school buildings were considered in the analyses. Additionally, the non-retrofitted conditions of these four school buildings were also examined through nonlinear time history analyses. Earthquake accelerations obtained from the nearest stations to the school buildings were used in these analyses. The satellite views of schools and accelerometer stations, along with the distances between them, are provided in Fig. 15. School-1 and School-2 are located in the Dulkadiroğlu district, while School-3 and School-4 are situated in the Onikişubat district. In this context,

Table 2 Some information on the examined school structures

School name	District	Retrofitting situation	Damage status	Construction year	Story	Concrete grade (MPa)	Rebar grade	Foundation system	Soil properties
School 1 A Block	Dulkadiroğlu	Retrofitted	No damage	–	3	7.0	StI	Continuous	Z4
School 1 B Block	Dulkadiroğlu	Retrofitted	No damage	–	4	7.0	StI	Continuous	Z4
School 2 A Block	Dulkadiroğlu	Retrofitted	No damage	1993	4	6.8	StI	Continuous	ZD
School 2 C Block	Dulkadiroğlu	Retrofitted	No damage	1993	4	6.8	StI	Continuous	ZD
School 3 A Block	Onikişubat	Retrofitted	No damage	2005	3	24.9	StIII	Continuous	ZD
School 3 C Block	Onikişubat	Retrofitted	No damage	2005	4	18.3	StIII	Continuous	ZD
School 4	Onikişubat	Retrofitted	Slight damage	2004	3	12.5	StI	Continuous	ZC

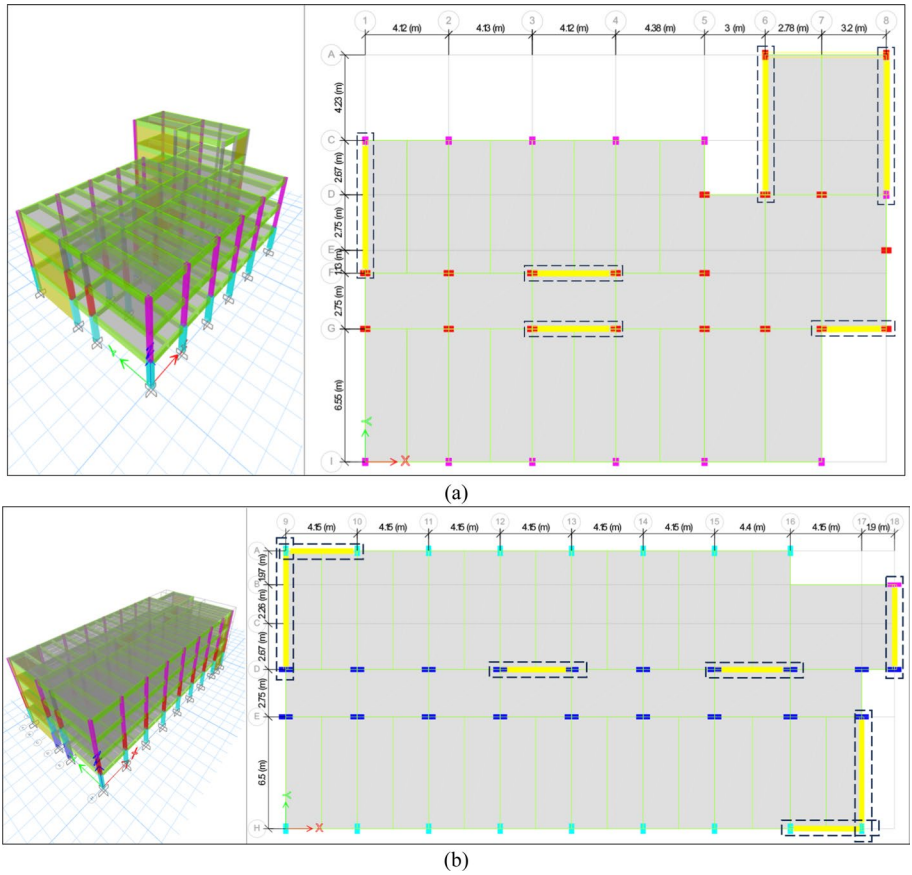

Fig. 14 Formwork plans and 3D views for retrofitted school structures: **a** school 1 A block, **b** school 1 B block, **c** school 2 A block, **d** school 2 C block, **e** school 3 A block, **f** school 3 C block, **g** school 4

accelerometers with station codes 4624 (Onikişubat) and 4625 (Dulkadiroğlu) have been utilized. Additionally, the acceleration records for the district of Pazarcık, which is the epicenter of the earthquake in question, were obtained from station 4614. Onikişubat and Dulkadiroğlu are neighboring districts. The maximum ground acceleration (PGA) recorded at the accelerometer stations occurred in Pazarcık, reaching 2178.72 cm/s^2. Following Pazarcık, Dulkadiroğlu recorded 466.33 cm/s^2, and Onikişubat recorded 357.25 cm/s^2. The acceleration records in two perpendicular horizontal directions were simultaneously applied to the structural system's principal axes (X) and (Y). The results obtained from the analyses were evaluated by taking the average of the absolute values of the maximum values. The acceleration records in Figs. 16, 17 and 18a, b and Table 3 were obtained from Turkish Accelerometric Database and Analysis System of the Disaster and Emergency Management Presidency (AFAD). The design spectrum and response spectrum for the relevant earthquakes are presented in Fig. 16, 17 and 18c. The design spectrum in the graphs were developed based on the location of school buildings and approximate site classes, considering the TBEC-2018 conditions. The response spectrum were obtained by utilizing the maximum values of building accelerations against ground motions for structures with

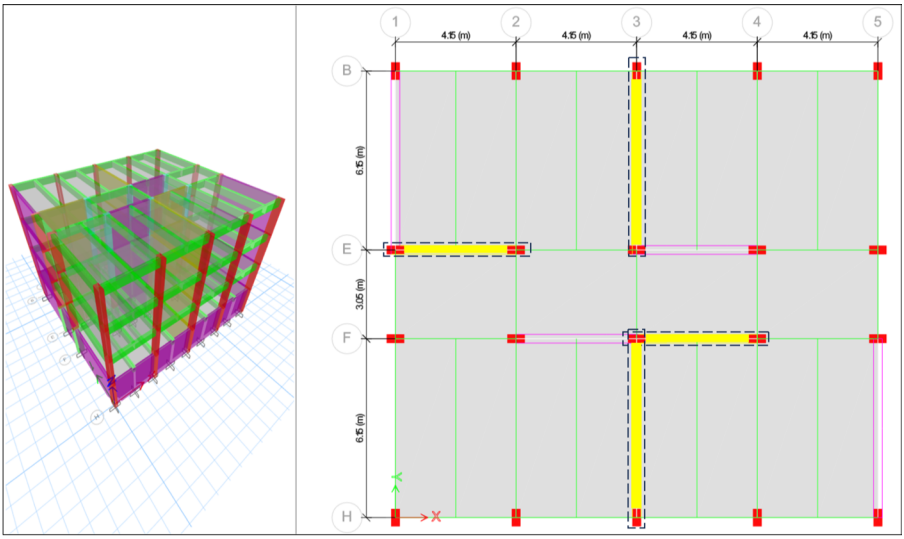

(c)

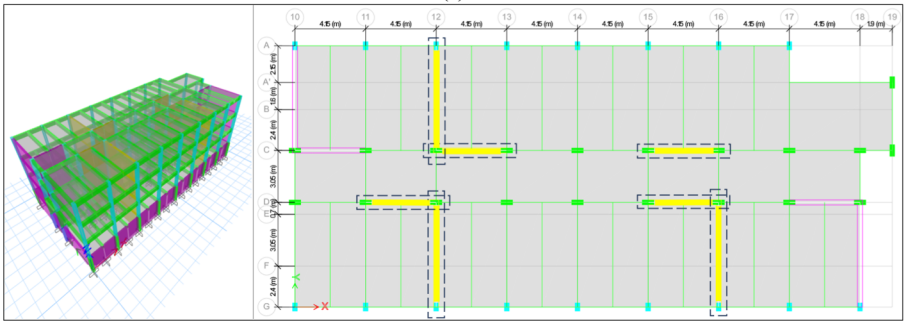

(d)

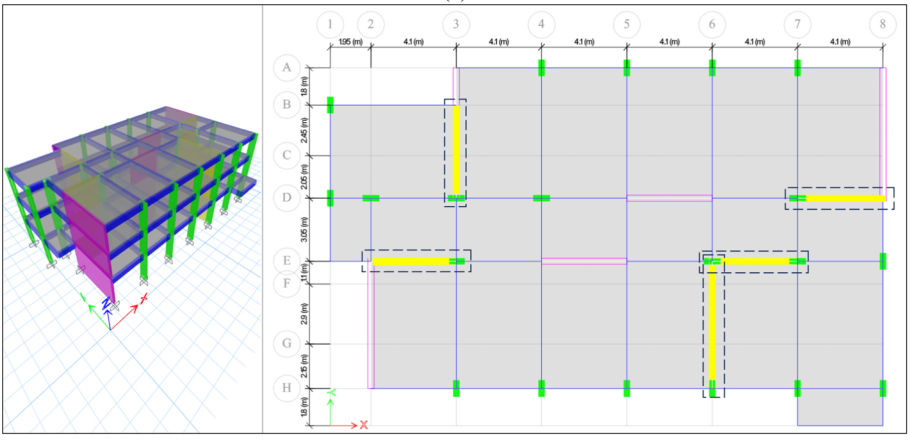

(e)

Fig. 14 (continued)

single-degree-of-freedom systems and different natural periods, all with a fixed damping

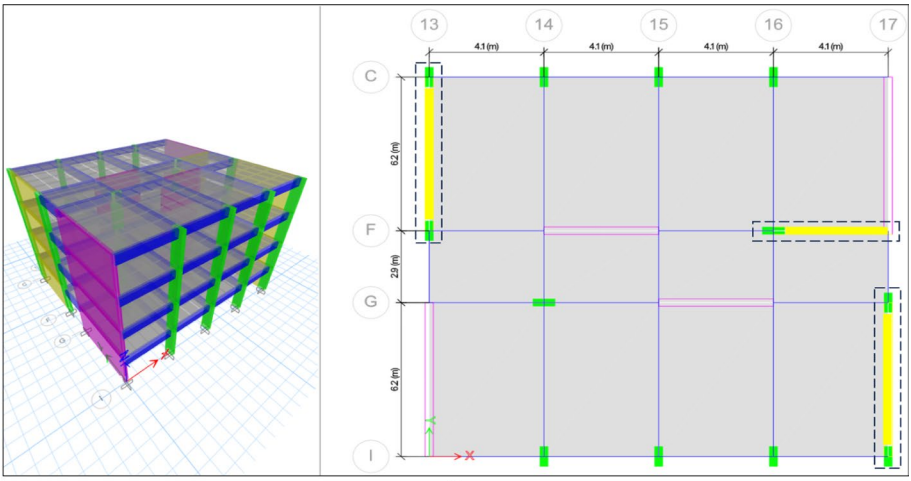

(f)

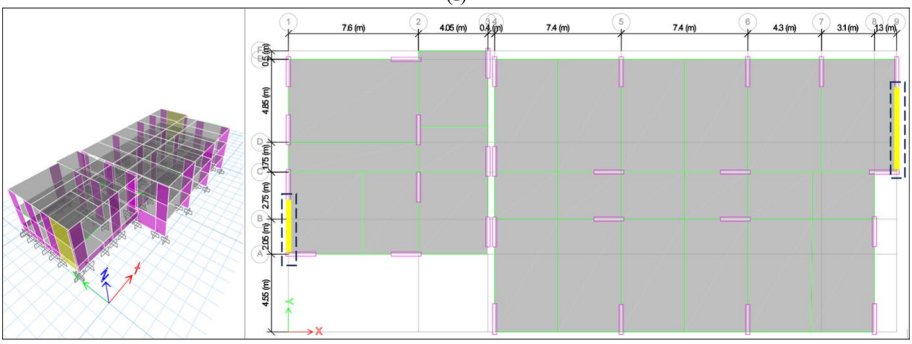

(g)

Fig. 14 (continued)

ratio. In Pazarcık, especially in low and medium-rise structures, the response spectrum have exceeded the design spectrum. In Dulkadiroğlu and Onikişubat, the design spectrum is relatively higher than response spectrum of earthquakes (Figs. 17, 18).

2.2.2 Nonlinear behavior models

To perform nonlinear analyzes of structures, certain nonlinear behavior models are defined for structural elements. These behavior models are concentrated or distributed plastic behavior models for columns, beams and shear walls, as stated in TBEC-2018. Many structural elements can be modelled with various plastic hinge models, as shown in Fig. 19. In the study, fiber plastic hinges are assigned to Lp = 0.5 h from the start and end points of the column and beam elements, forming 15% of the relative length of the element (Fig. 19c). Plastic hinges are defined as P-M2-M3 for columns and beams. P-M3 auto fiber wall plastic hinges are assigned to the shear walls we mesh (Fig. 19e). A plastic hinge was assigned to each shear wall and the maximum strains in the elements were evaluated. The fiber section plastic hinge model distributes plasticity along the length and cross-section of the element through numerical integrations. This model

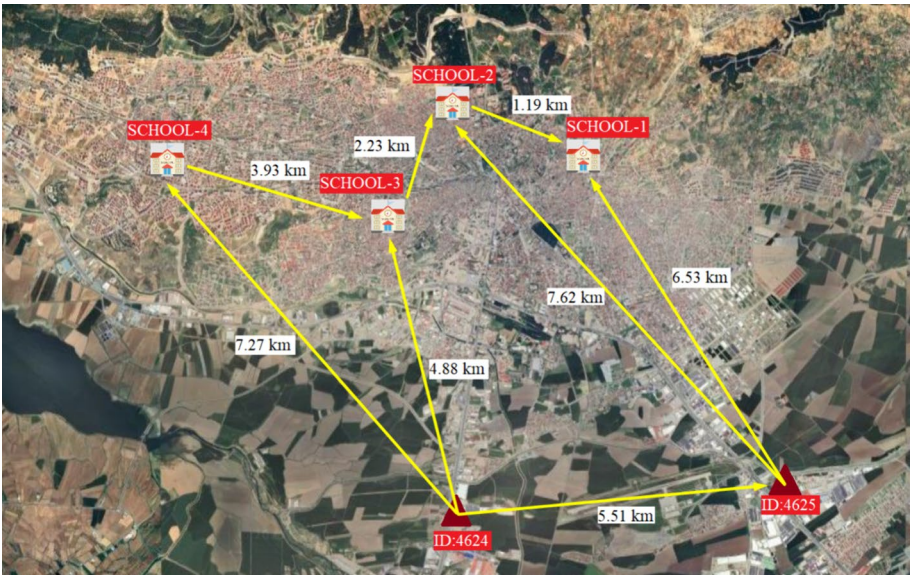

Fig. 15 Accelerometer stations and the schools of satellite views

does not report rotations on the element; instead, it reports strain and stresses. We calculated the strain limit values given in TBEC 2018 and compared them with these reported values.

The significant differences between the existing shear walls in the structure and the retrofitted shear walls involve stirrup spacing, rebar diameter, and concrete class. While the stirrup spacing in the existing shear walls is 20 cm, it has been reduced to 10 cm in the retrofitted shear walls. Additionally, as evident from Table 4, the concrete class of the shear walls is significantly higher than that of the existing ones.

2.2.3 Performance-based design

The strain of the fiber materials in the fiber plastic hinge section of the members was determined using the ETABS program. These strains were compared with the boundary conditions specified in Eqs. 2–10 of TBEC 2018. Damage zones depending on the boundary conditions are given in Fig. 20. Three limit conditions have been defined for ductile elements on the cross section. These are Minimum Damage Limit (IO), Life Safety Limit (LS) and Collapsing Limit (CP). Minimum damage limit defines the beginning of the behavior beyond elasticity, safety limit defines the limit of the behavior beyond elasticity that the section is capable of safely ensuring the strength, and collapsing limit defines the limit of the behavior before collapsing. This classification does not apply to elements damaged in a brittle condition. In Fig. 20 elements that the damages with critical sections do not reach IO are within the Minimum Damage Region, those in-between IO and LS are within Moderate Damage Region, those in-between LS and CP are in Heavy Damage Region, and those going beyond CP are within Collapsing Region.

Strain limits for concrete material;

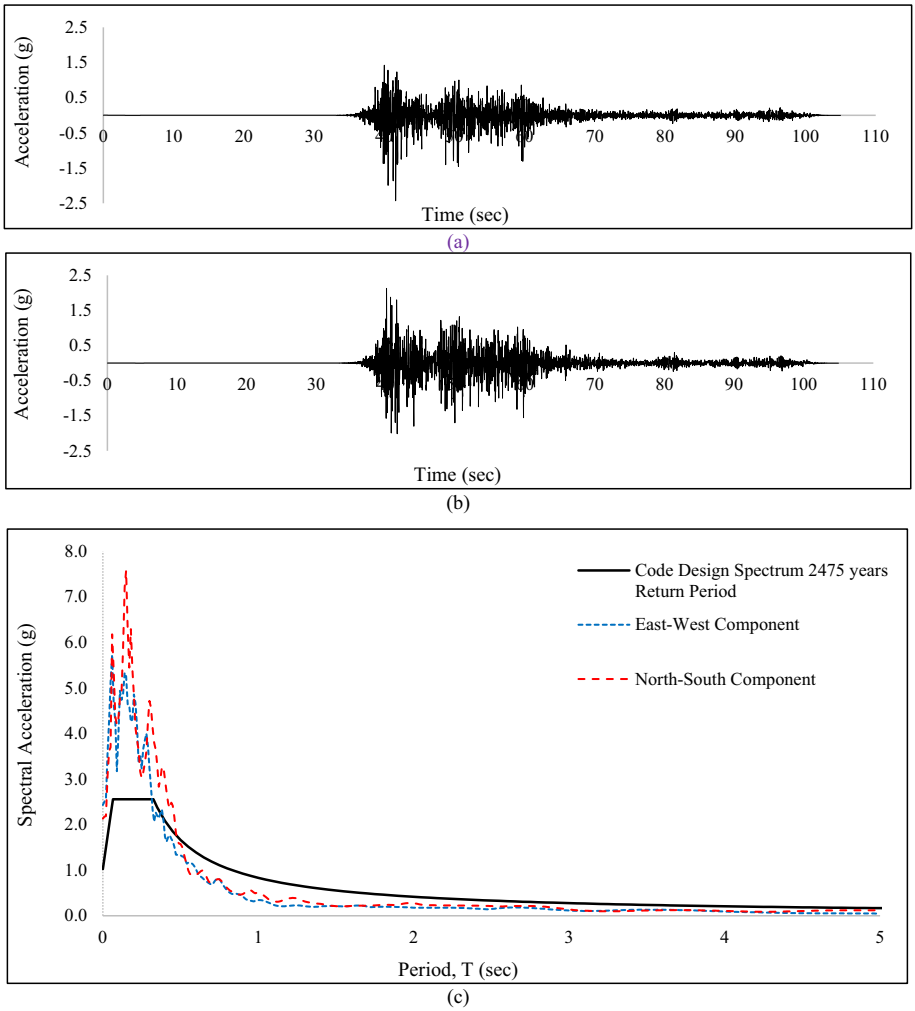

Fig. 16 The largest acceleration record from the 4614 station of the Pazarcık earthquake; **a** east–west component, **b** north–south component, **c** response spectrum

$$\varepsilon_c^{(CP)} = 0.0035 + 0.04\sqrt{\omega_{we}} \leq 0.018 \tag{2}$$

here, ω_{we} represents the ratio of effective stirrup bar to mechanical reinforcement and is formulated as follows;

$$\omega_{we} = \alpha_{se}\rho_{sh,min}\frac{f_{ywe}}{f_{ce}} \tag{3}$$

here α_{se} shows the stirrup bar efficiency coefficient and is formulated as follows. $\rho_{sh,min}$ shows the smaller of the volumetric stirrup bar ratio in two horizontal directions in a rectangular section and is formulated as follows, f_{ywe} shows the average (expected) yield strength of stirrup bar;

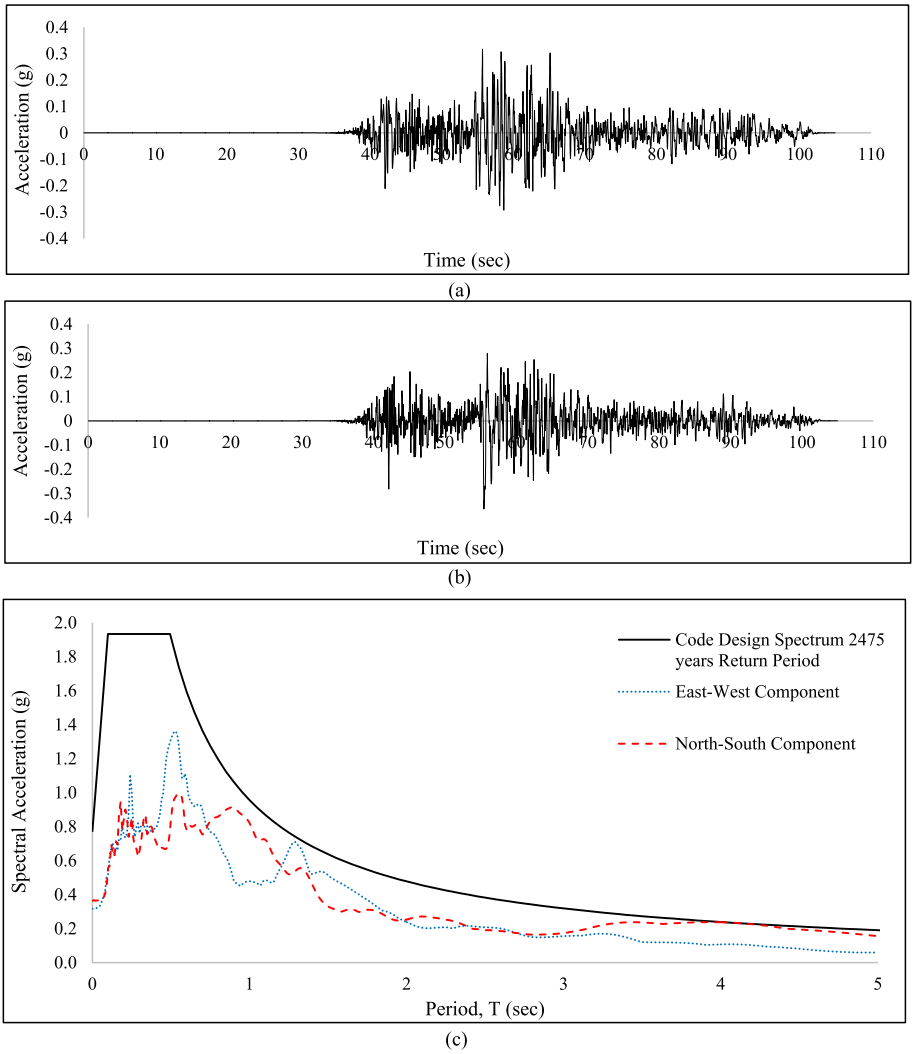

Fig. 17 Acceleration record from Onikisubat district 4624 station of the Pazarcık earthquake; **a** east–west component, **b** north–south component, **c** response spectrum

$$\alpha_{se} = \left(1 - \frac{\sum a_i^2}{6b_o h_o}\right)\left(1 - \frac{s}{2b_o}\right)\left(1 - \frac{s}{2h_o}\right) \tag{4}$$

$$\rho_{sh} = \frac{A_{sh}}{b_k s} \tag{5}$$

A_{sh} and ρ_{sh} represent the area and volumetric ratio of the stirrup bar considered, respectively. b_k denotes the core dimension in the perpendicular direction (distance between the outermost stirrup bar axes), s represents the spacing of the stirrup bar, b_o and h_o denote the dimensions of the confined concrete measured from the axes of the stirrup bar, and

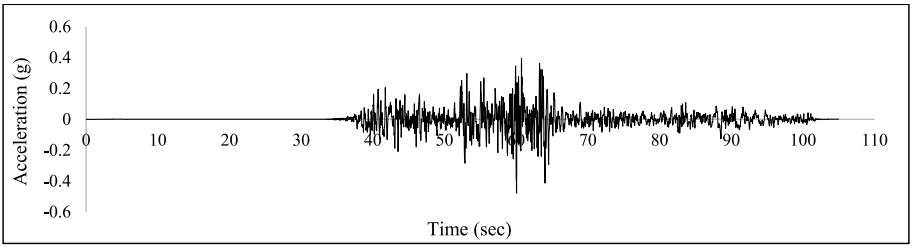

(a)

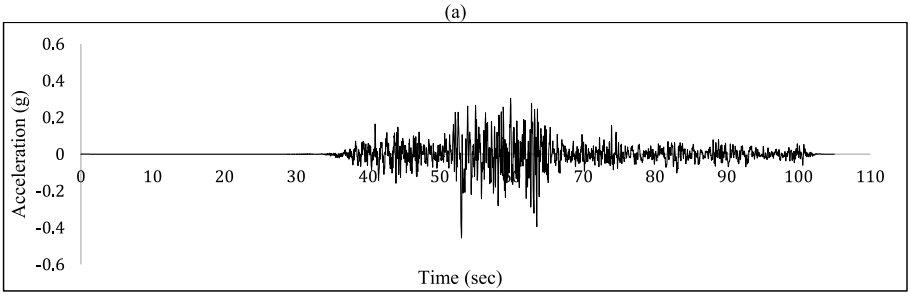

(b)

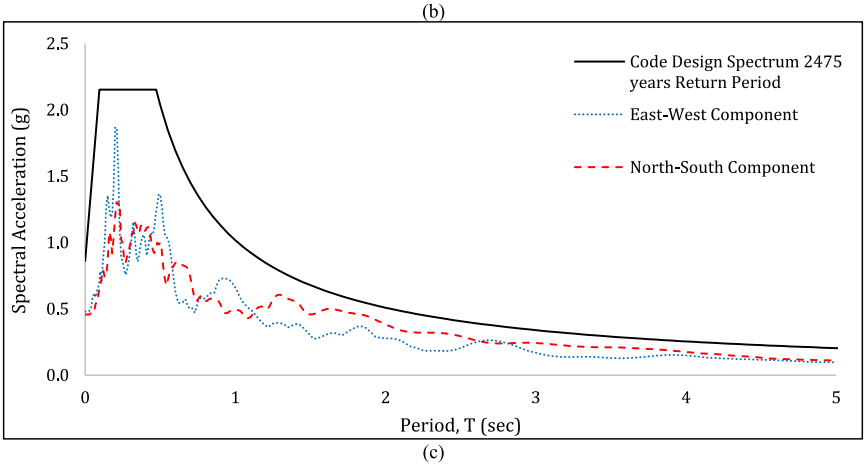

(c)

Fig. 18 Acceleration record from Dulkadiroğlu district 4625 station of the Pazarcık earthquake; **a** east–west component, **b** north–south component, **c** response spectrum

Table 3 Information on acceleration records

Accelerogram	Record station	PGA (g)	Vs30 (m/s)	Max acceleration (g)	Max velocity (m/s)	Max displacement (m)	Significant duration (s)	Magnitude
Onikişubat	4624	0.784	280	0.364	0.59	0.377	45.29	7.7
Dulkadiroğlu	4625	0.870	346	0.475	0.757	0.463	41.90	7.7
Pazarcık	4614	0.853	541	2.22	0.94	0.945	22.25	7.7

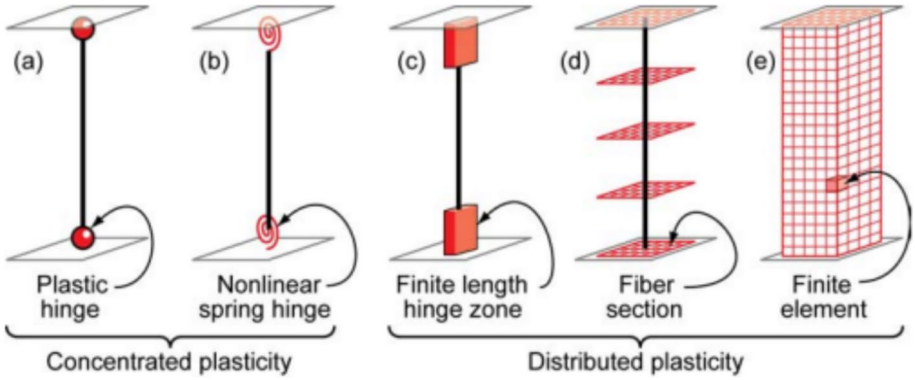

Fig. 19 Various nonlinear behavior models usable in structural elements (Deierlein et al. 2010)

Table 4 Retrofitted and non-retrofitted material grades

School name	Non-retrofitted		Retrofitted	
	Concrete grade (MPa)	Rebar grade	Concrete grade (MPa)	Rebar grade
School 1 A Block	7.0	StI	20	S420
School 1 B Block	7.0	StI	20	S420
School 2 A Block	6.8	StI	30	STIII
School 2 C Block	6.8	StI	30	STIII
School 3 A Block	24.9	StIII	30	STIII
School 3 C Block	18.3	StIII	30	STIII
School 4	12.5	StI	30	S420

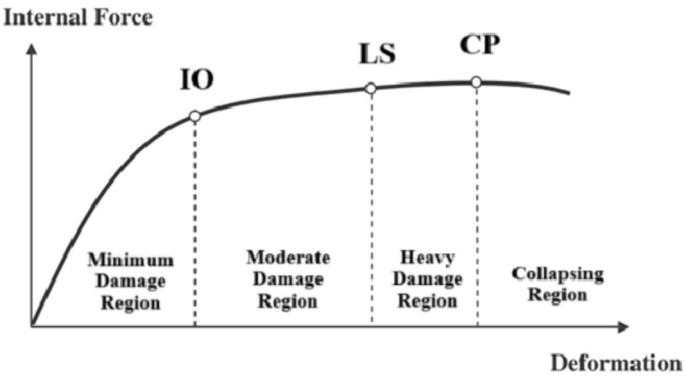

Fig. 20 Damage zones

a_i indicates the distance between the longitudinal reinforcement axes supported by stirrup arm.

$$\varepsilon_c^{(LS)} = 0.75\varepsilon_c^{(CP)} \tag{6}$$

$$\varepsilon_c^{(IO)} = 0.0025 \tag{7}$$

strain limits for rebar material;

$$\varepsilon_s^{(CP)} = 0.4\varepsilon_{su} \tag{8}$$

$$\varepsilon_s^{(LS)} = 0.75\varepsilon_s^{(CP)} \tag{9}$$

$$\varepsilon_s^{(IO)} = 0.0075 \tag{10}$$

2.2.4 Concrete and reinforcement steel material models

The concrete model used in the study was defined based on the mander concrete model (Mander et al. 1988), as in TBEC 2018 Annex 5A. The reinforcing steel model was defined according to TBEC 2018 Annex 5A, taking into account the hardening effect. The elasticity modulus of the reinforcing steel is taken as $E_S = 2 \times 10^5$ MPa. Figure 16 shows the stress strain curves of concrete and reinforcing steel. In Fig. 21, f_{cc} indicates the strength of confined concrete, f_{co} denotes the strength of unconfined concrete, f_{su} represents the fracture strength of the reinforcement steel, and f_{sy} signifies the yield strength of the reinforcement steel.

3 Results

3.1 Natural periods of structures

The natural vibration periods resulting from the modal analysis of the structures are presented in Table 5. The natural vibration periods of the retrofitted structures have decreased significantly compared to the non-retrofitted situation. The addition of shear walls has increased the structural rigidity of the building. As a result, the period values have decreased. Rigidity and period develop inversely proportional to each other. In addition,

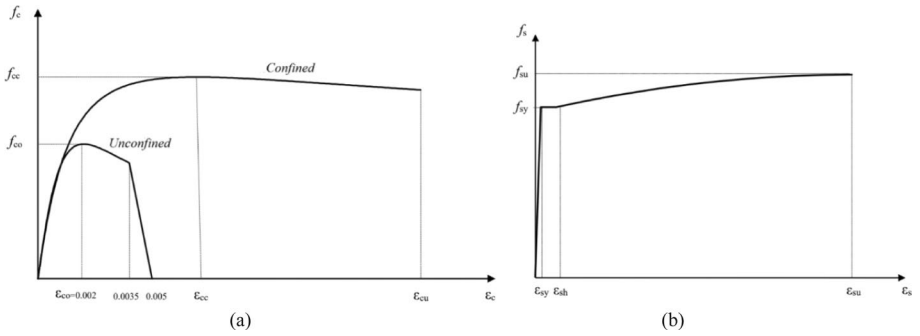

Fig. 21 Material models: **a** concrete model, **b** reinforcing steel model

Table 5 Periods of non-retrofitted and retrofitted conditions of the school structures subject to investigation

School name	Non-retrofitted structure period (s)			Retrofitted structure period (s)		
	X	Y	TpE	X	Y	TpE
School 1 A Block	0.65	0.76	0.69	0.19	0.15	0.48
School 1 B Block	0.73	0.91	0.64	0.28	0.22	0.45
School 2 A Block	0.33	0.24	0.50	0.20	0.15	0.50
School 2 C Block	0.32	0.23	0.50	0.21	0.15	0.50
School 3 A Block	0.30	0.21	0.41	0.18	0.13	0.41
School 3 C Block	0.34	0.24	0.48	0.25	0.15	0.48
School 4	0.35	0.24	0.37	0.34	0.22	0.37

period values were compared with empirical natural period values in TBEC-2018. Equation 11 indicates the empirical natural period given in TBEC-2018. Here, C_t is the coefficient used in the calculation of the empirical natural period (The load-bearing system will be taken Ct = 0.1 in buildings consisting only of RC frames, Ct = 0.08 in buildings consisting of steel frames or steel frames with cross, Ct = 0.07 in all other buildings), and H_N is the total height of the upper part of the building above the basement story. The highest value of the calculated natural period of the building to be taken into account in the earthquake calculation will not be more than 1.4 times the TpE period.

$$T_{pE} = C_t H_N^{3/4} \tag{11}$$

According to the data in Table 5, the structural retrofitting process resulted in a decrease in the structure periods of school 1 A and B blocks. In the x-direction, the structure period of the A block decreased by 70.77%, while the structure period of the B block decreased by 61.64%. In the y-direction, the structure period of the A block decreased by 80.26%, and the structure period of the B block decreased by 75.82%. In school 2 A and C blocks, a decrease of 39.39% and 34.38% was observed in the x-direction, respectively. In the y-direction, the structure period of the A block decreased by 37.5%, while the structure period of the C block decreased by 34.78%. In school 3 A and C blocks, a decrease of 40% and 26.47% was observed in the x-direction, respectively. In the y-direction, the structure period of the A block decreased by 38.09%, while the structure period of the C block decreased by 37.5%. Finally, in the school 4 building, a decrease of 2.86% and 8.33%, respectively, was observed in the x and y-directions.

3.2 Story displacements

School structures are located in the Dulkadiroğlu and Onikişubat districts. Analyses were conducted using the N–S and E–W components of records obtained from stations in these two districts. These components show similar values for each earthquake. Simulations were performed using these records, and the maximum responses occurring during the recordings were reported. As a result of nonlinear time history analyses, it was observed that retrofitted structures exhibited significant reductions in story displacements compared to non-retrofitted structures. The results obtained are shown in Fig. 22 as graphs containing the maximum values of the positive and negative directions of x and y. The final ratios

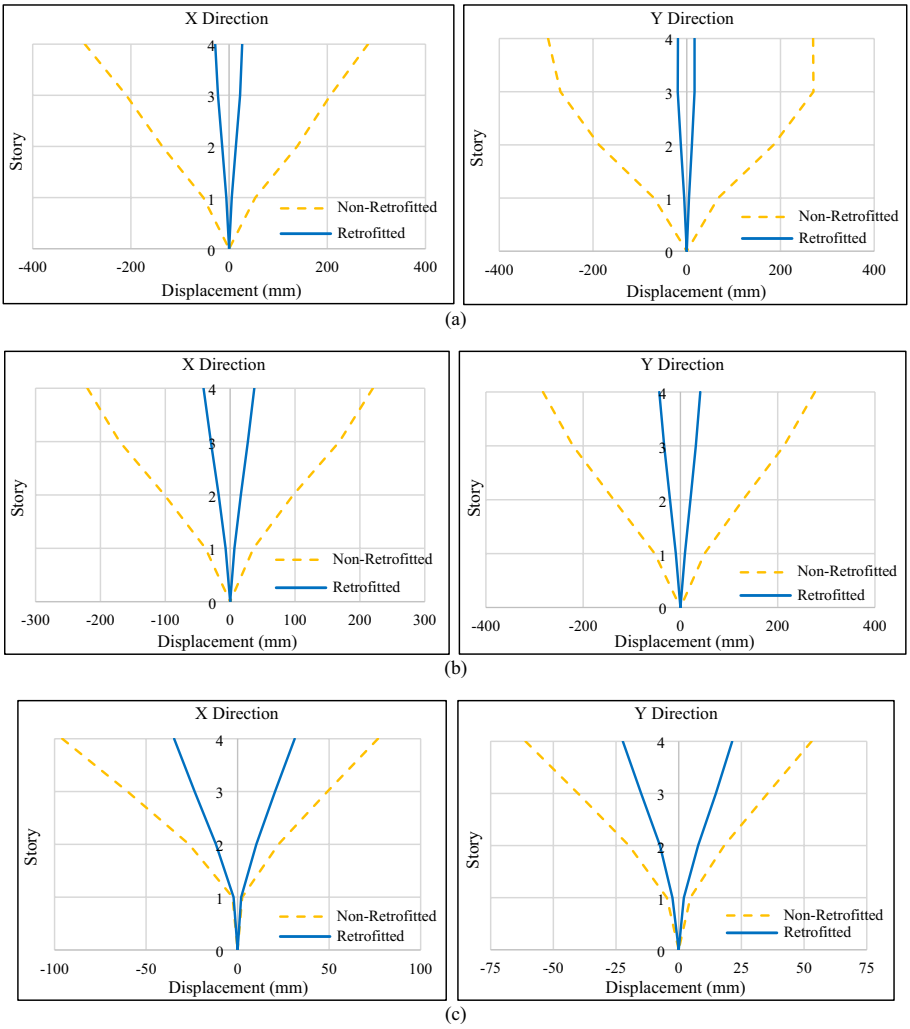

Fig. 22 Story displacements of examined school buildings: **a** school 1 A block, **b** school 1 B block, **c** school 2 A block, **d** school 2 C block, **e** school 3 A block, **f** school 3 C block, **g** school 4

were calculated based on the maximum absolute values. Looking at the extreme examples, the roof displacement in school 1 A block decreased by 93.66%, while it increased by 4.06% in school 4 T2.

According to the graphs, significant decreases in roof displacement have been observed in the retrofitted structures compared to the non-retrofitted structures. In school 1 A and B blocks, roof displacement has decreased by %90.36 and %81.34 in the x direction and %93.66 and %84.62 in the y direction, respectively. In school 2 A and C blocks, roof displacement has decreased by %63.77 and %55.69 in the x direction and %63.53 and %55.62 in the y direction, respectively. In school 3 A and C blocks, roof displacement has decreased by %81.23 and %47.69 in the x direction and %59.22 and %59.63 in the y direction, respectively. Finally, in school 4 T1 and T2 blocks, there has

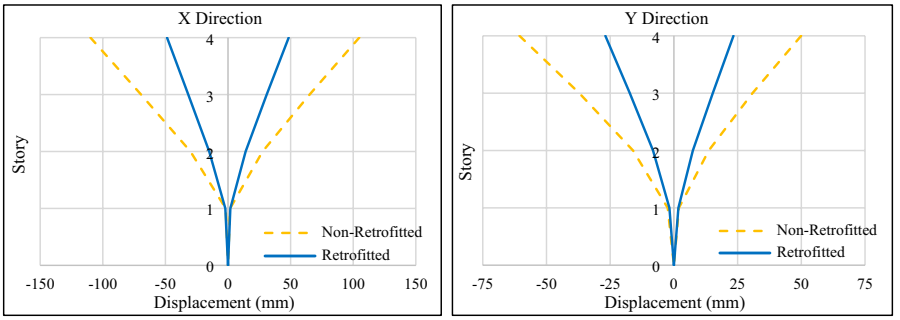

(d)

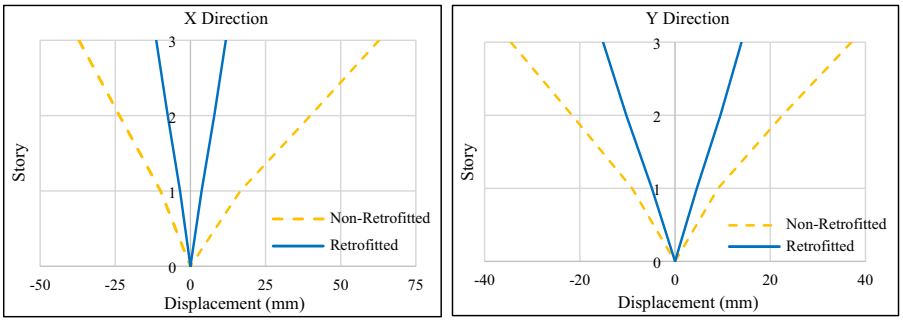

(e)

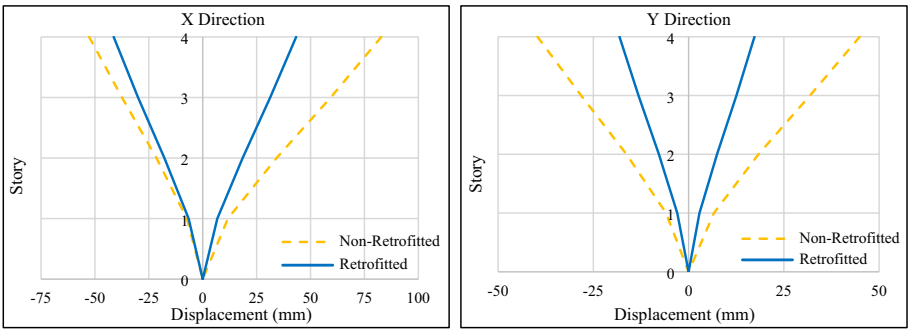

(f)

Fig. 22 (continued)

been a decrease of 11.15% in the x direction in both blocks. In the y direction, there has been an increase of 4.06% in T1 and a decrease of 26.20% in T2.

In retrofitting, if shear walls are used in effective directions and in sufficient numbers, they can significantly reduce story displacements with the rigidity they add to structural systems. Therefore, in some structures where there is not a significant need for retrofitting, significant changes are not observed, while in structures where retrofitting is essential, significant alterations have been seen as a result of the retrofitting process. All structures except School Building 4 have been retrofitted with sufficient shear wall elements in both directions, resulting in significant reductions in story displacements in both directions. However, School Building 4 has been retrofitted with a total of 2 shear walls, with one for each block in one direction.

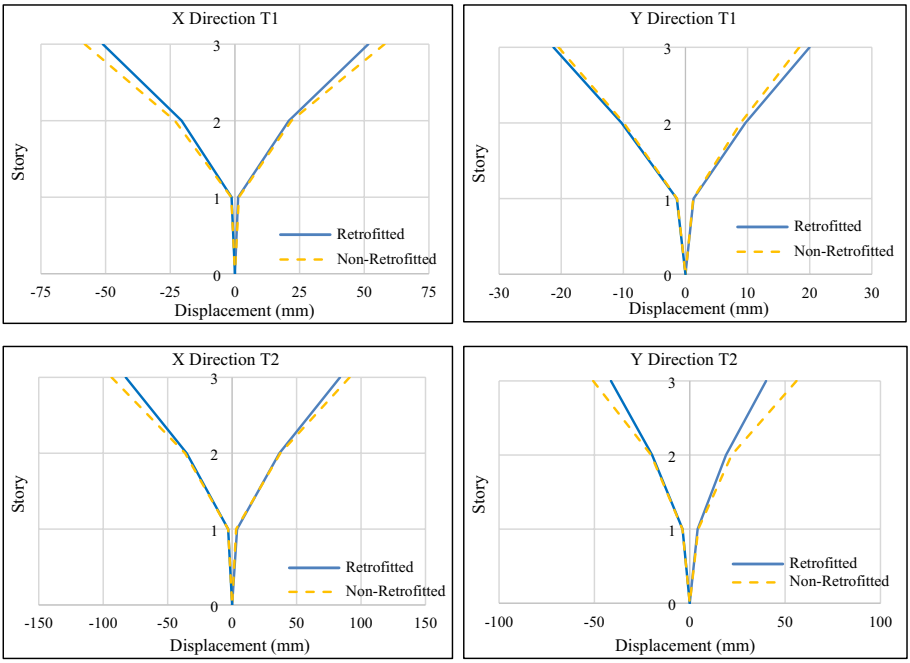

Fig. 22 (continued)

3.3 Story drifts

Field observations and FEA have revealed that, in non-retrofitted conditions, interstory drifts exceed the code limits. This indicates insufficient lateral rigidity in the structures. In cases of such structural issues, retrofitting applications with cast-in-place RC shear walls have been observed to yield successful results in enhancing both the lateral rigidity and strength of the structures (TBEC-2018). Table 6 presents the drift percentages in the x and y directions for the retrofitted and non-retrofitted states of the schools. According to the Türkiye

Table 6 The largest drifts of the non-retrofitted and retrofitted state of the school buildings that are the subject of the study

School name	Non-retrofitted drift (%)		$\lambda\frac{\delta_{i,max}^{(X)}}{h_i} \le 0.008\kappa$				Retrofitted drift (%)		$\lambda\frac{\delta_{i,max}^{(X)}}{h_i} \le 0.008\kappa$			
	X	Y	X		Y		X	Y	X		Y	
School 1 A Block	3.47	3.58	0.093	X	0.089	X	0.26	0.22	0.007992	✓	0.005328	✓
School 1 B Block	2.42	3.16	0.059	X	0.079	X	0.4	0.4	0.010656	X	0.010656	X
School 2 A Block	1.05	0.62	0.028	X	0.016	X	0.34	0.22	0.005832	✓	0.003888	✓
School 2 C Block	1.2	0.7	0.031	X	0.018	X	0.52	0.28	0.00972	X	0.005832	✓
School 3 A Block	0.71	0.44	0.018	X	0.01	X	0.13	0.16	0.001944	✓	0.003888	✓
School 3 C Block	0.76	0.41	0.021	X	0.01	X	0.39	0.16	0.007776	✓	0.003888	✓
School 4 T1	1.17	0.35	0.023	X	0.009	X	1.04	0.36	0.0144	X	0.006416	✓

Seismic Code-2007 (TSC-2007) earthquake regulations, interstory drift values of approximately 1% indicate the onset of slight damage, while levels around 2% suggest significant damage. According to TBEC-2018, there are limit conditions for interstory drift. The control of displacements in both directions for schools is conducted in Table 6. In this table, λ represents the empirical coefficient used to limit interstorey drifts, while κ denotes the coefficient used differently for defining permissible interstorey drifts in RC and steel structural systems. δ stands for the interstorey drift value, whereas h represents the story height value. The conditions where the checks are satisfied are indicated by "✓," and cases where they are not satisfied are represented by "X". In the non-retrofitted condition of all school buildings, the condition of interstory drift has not been satisfied in either direction. As a result of the retrofitting of the schools, however, the values of interstory drift have decreased in all buildings. If the school 1 A and B Block structures had not been retrofitted, these structures could likely have experienced significant displacements and drifts. As a result, the structures could have potentially suffered severe damage or even collapsed. The retrofitting measures effectively prevented severe damage and collapse by significantly reducing the displacements and drifts in both blocks. The fact that the reinforced school 1 A and B Block structures did not suffer any damage in the earthquake further validates the effectiveness of the retrofitting approach. Despite the retrofitting, the school 4 structure still experienced a drift level of 1.65% in the x-direction. On-site inspections revealed that the school 4 structure survived these earthquakes with minor wall damage. Numerical calculations have determined that the other retrofitted school structures could have also survived the earthquakes with minor damage even if they had not been retrofitted. Consistent with the numerical analyses, no damage was observed in these structures. When evaluated under TBEC 2018 conditions, despite the reinforcement application, School 1 Block B has not met the boundary conditions in both directions, School 2 Block C, and School 4 in the x direction.

According to the data in Table 6, there was a significant decrease in story drifts after the building retrofitting process. Specifically, in school 1 A block, there was a decrease of 92.51% in the x-direction and 93.85% in the y-direction. In the B block, the decrease was 83.47% in the x-direction and 87.34% in the y-direction. In school 2 A and C blocks, there was a decrease of 67.62% and 56.67%, respectively, in the x-direction, and a decrease of 64.52% and 60%, respectively, in the y-direction. In school 3 A and C blocks, there was a decrease of 81.69% and 48.68%, respectively, in the x-direction, and a decrease of 63.64% and 60.98%, respectively, in the y-direction. Finally, in school 4 T1 and T2, there was a decrease of 11.11% and 10.81%, respectively, in the x-direction. In the y-direction, there was an increase of 2.86% in T1 and a decrease of 37.39% in T2.

3.4 Seismic energy input to the buildings

The input seismic energy was obtained separately for each structure by extracting earthquake data from the display-show tables section of the ETABS program, based on the nearest station where the record was taken. Since the structural rigidity has increased with the addition of shear walls to school buildings, it has significantly reduced the amount of energy entering the building. As a result of the decrease in earthquake energy entering the building, the amount of energy converted into irrecoverable hysteretic energy also decreased significantly (Table 7).

Specifically, for school 1 A Block, the decrease was 84.62%. For school 1 B Block, it was 63.7%. School 2 A Block experienced a decrease of 43.71%, school 2 C Block had a

Table 7 Seismic input energies of examined school buildings in retrofitted and non-retrofitted states

School name	Non-retrofitted structure Input energy (kN-m)	Retrofitted structure Input energy (kN-m)
School 1 A Block	14,796.26	2276.26
School 1 B Block	27,195.61	9872.56
School 2 A Block	8478.63	4772.52
School 2 C Block	13,117.28	6388.00
School 3 A Block	5281.36	1671.68
School 3 C Block	4469.39	2726.69
School 4	6690.92	6213.16

decrease of 51.28%, school 3 A block had a decrease of 68.35%, school 3 C block had a decrease of 38.99%, and school 4 experienced a decrease of 7.14%.

3.5 Performance based design results

Nonlinear time history analyses of each school building in both their retrofitted and non-retrofitted states were performed using the ETABS program according to the TBEC-2018. The analyses aimed to assess the response of the structures under earthquake loading and determine the resulting damage to the column, beam, and shear wall elements. The damage to structural elements of the school buildings is given in Tables 8 and 9. Tables 8 and 9 illustrate the minimum damage region as MiD, the moderate damage region as MoD, the heavy damage region as HD, and the collapsing region as CR.

Before the earthquake, school structures were subjected to performance analysis and retrofitted through package programs using the design spectrum data obtained from the Earthquake Hazard Map of Turkey. The earthquake data affecting school structures, as shown in Figs. 17 and 18, are below the design spectrum. Therefore, the structures were minimally impacted by the maximum acceleration values of the earthquake specified in Fig. 16. The buildings have the capacity to withstand this earthquake with little or no damage, either with or without retrofitting.

According to the results of the nonlinear time history analyses, it was determined that the school 1 A and B block structures would have suffered significant damage if they had not been retrofitted before the earthquakes. If this school had not been retrofitted, numerous column elements belonging to A and B blocks could have reached the Moderate Damage Region and Heavy Damage regions and suffered damage. However, no such problem was encountered in the other school buildings, both retrofitted and non-retrofitted. This situation can be attributed to the positive parameters mentioned above for schools.

4 Conclusions

Many cities experienced significant loss of life and extensive building collapses as a consequence of earthquakes. The primary cause of these losses is not the earthquakes themselves, but rather the buildings that have insufficient earthquake resilience. Especially

Table 8 Damage to structural elements in non-retrofitted schools resulting from nonlinear time history analyses

School name	Non-retrofitted											
	Column				Beam				Shear wall			
	MiD%	MoD%	HD %	CR %	MiD%	MoD%	HD %	CR %	MiD%	MoD%	HD%	CR %
School 1 A Block	0.98	86.27	12.75	0	100	0	0	0	None			
School 1 B Block	0	76.35	23.65	0	100	0	0	0	None			
School 2 A Block	100	0	0	0	100	0	0	0	100	0	0	0
School 2 C Block	100	0	0	0	100	0	0	0	96.81	1.87	0	0
School 3 A Block	100	0	0	0	100	0	0	0	100	0	0	0
School 3 C Block	100	0	0	0	100	0	0	0	100	0	0	0
School 4	None				100	0	0	0	94.34	5.66	0	0

Table 9 Damage to structural elements in retrofitted schools resulting from nonlinear time history analyses

School name	Retrofitted											
	Column				Beam				Shear wall			
	MiD%	MoD%	HD %	CR %	MiD%	MoD%	HD %	CR %	MiD%	MoD%	HD%	CR %
School 1 A Block	100	0	0	0	100	0	0	0	100	0	0	0
School 1 B Block	100	0	0	0	100	0	0	0	100	0	0	0
School 2 A Block	100	0	0	0	100	0	0	0	100	0	0	0
School 2 C Block	100	0	0	0	100	0	0	0	100	0	0	0
School 3 A Block	100	0	0	0	100	0	0	0	100	0	0	0
School 3 C Block	100	0	0	0	100	0	0	0	100	0	0	0
School 4	None				100	0	0	0	94.69	5.31	0	0

before the year 2000, it was observed that buildings in earthquake areas suffered significant damage or collapsed. The following defects were observed in many of the school structures in the earthquake region:

- Column dimensions were selected to be brittle,
- The use of shear walls was not common,
- There were problems with adherence and development length,
- Use of rebar without ribs and with low yield strength,
- Stirrup spacing was excessive and the 90° hook was commonly used,
- Segregation problem that negatively affects the physical and mechanical properties of concrete
- Concrete quality was poor,
- Soft story conditions existed,

In the scope of the study, field observations conducted in the earthquake-prone area revealed that the most common problems leading to structural collapses in school buildings are inadequate adherence, development length mechanisms and stirrup spacing. Subsequently, inadequate column sizes and concrete quality can be listed. The implementation of retrofitting techniques such as RC shear walls methods has proven to significantly enhance the seismic resilience of buildings, effectively mitigating the impact of earthquakes. In the inspected retrofitted schools, significant damage was not observed in the structural elements. Damage states of the retrofitted structures were obtained by numerical analyses in this study. As a result of numerical analyses, it was simulated that the retrofitted structures did not suffer any damage. Only in the case of school 1 buildings, if they had not been retrofitted before the earthquakes, it is predicted that these structures could have suffered damage during the earthquakes. During the numerical examination of school buildings in earthquake areas, it was observed that the existing shear walls in the structures played a vital role in maintaining the structural integrity of the buildings during seismic events. Additionally, the introduction of shear walls resulted in a decrease in the energy transmitted to the buildings. Moreover, the inclusion of shear walls significantly reduced the displacements and drifts of the building stories. This finding highlights the effectiveness of shear walls in enhancing the seismic performance of school buildings. Both field studies and numerical analyses have yielded a crucial understanding that school buildings, despite having highly inadequate material details, can withstand even severe earthquakes without collapsing if they undergo proper retrofitting with suitable methods. This significant insight emphasizes the importance of implementing appropriate retrofit measures to enhance the seismic resilience of such buildings.

Acknowledgements We would like to acknowledge the partial funding received for our fieldwork from the 1002-C Natural Disasters-Focused Fieldwork Emergency Support Program by The Scientific and Technological Research Institution of Türkiye (TÜBİTAK).

Author contribution All authors have contributed to the writing of the manuscript. AD and TYA were involved in field explorations in the earthquake-prone region, while MŞ took part in conducting the analyses. All authors have read, reviewed, and approved the final manuscript.

Funding Openaccess funding provided by the Scientific and Technological Research Council of Türkiye(TÜBİTAK).

Conflict of interest The authors declare no conflict of interest.

Open Access This article is licensed under a Creative Commons Attribution 4.0 International License, which permits use, sharing, adaptation, distribution and reproduction in any medium or format, as long as

you give appropriate credit to the original author(s) and the source, provide a link to the Creative Commons licence, and indicate if changes were made. The images or other third party material in this article are included in the article's Creative Commons licence, unless indicated otherwise in a credit line to the material. If material is not included in the article's Creative Commons licence and your intended use is not permitted by statutory regulation or exceeds the permitted use, you will need to obtain permission directly from the copyright holder. To view a copy of this licence, visit http://creativecommons.org/licenses/by/4.0/.

References

Ahmad N, Akbar J, Rizwan M et al (2019) Haunch retrofitting technique for seismic upgrading deficient RC frames. Bull Earthq Eng 17:3895–3932. https://doi.org/10.1007/s10518-019-00638-9

Ahmad N, Masoudi M (2020) Eccentric steel brace retrofit for seismic upgrading of deficient reinforced concrete frames. Bull Earthq Eng 18:2807–2841. https://doi.org/10.1007/s10518-020-00808-0

Ahmad N, Shahzad A, Rizwan M et al (2017) Seismic performance assessment of non-compliant smrf reinforced concrete frame: shake table test study. J Earthq Eng. https://doi.org/10.1080/13632469.2017.1326426

Albanesi T, Biondi S, Candigliota E et al (2008) Seismic full-scale tests on a 3d infilled RC frame. In: 14th world conference on earthquake engineering, Beijing China

Almeida A, Ferreira R, Proença JM, Gago AS (2017) Seismic retrofit of RC building structures with Buckling Restrained Braces. Eng Struct 130:14–22. https://doi.org/10.1016/j.engstruct.2016.09.036

Altin S, Ersoy U, Tankut T (1992) Hysteretic response of reinforced-concrete infilled frames. J Struct Eng ASCE 118:2133–2150. https://doi.org/10.1061/(ASCE)0733-9445(1992)118:8(2133)

Altunişik A, Arslan M, Kahya V et al (2023) Field observations and damage evaluation in reinforced concrete buildings after the February 6th, 2023 Kahramanmaraş-Türkiye Earthquakes. J Earthq Tsunami. https://doi.org/10.1142/S1793431123500240

Altunişik A, Atmaca B, Kartal M et al (2021) Assessment of structural damage following the October 30, 2020 Aegean Sea Earthquake and Tsunami. J Earthq Tsunami 15:1–43. https://doi.org/10.1142/S1793431121500299

Atmaca B, Demir S, Günaydın M et al (2020) Lessons learned from the past earthquakes on building performance in Turkey. J Struct Eng Appl Mech 15:61–84

Bal İE, Gülay FG, Tezcan SS (2011) Use of analytical tools for calibration of parameters in P25 preliminary assessment method. In: Computational methods in earthquake engineering. Springer, pp 559–582

Bayraktar A, Altunişik AC, Pehlivan M (2013) Performance and damages of reinforced concrete buildings during the October 23 and November 9, 2011 Van, Turkey, earthquakes. Soil Dyn Earthq Eng 53:49–72. https://doi.org/10.1016/j.soildyn.2013.06.004

Belleri A, Brunesi E, Nascimbene R et al (2015) Seismic performance of precast industrial facilities following major earthquakes in the Italian Territory. J Perform Constr Facil 29:04014135. https://doi.org/10.1061/(ASCE)CF.1943-5509.0000617

Calvi GM (2013) Choices and criteria for seismic strengthening. J Earthq Eng 11:999–1019. https://doi.org/10.1080/13632469.2013.781556

Canbay E, Ersoy U, Ozcebe G (2003) Contribution of reinforced concrete infills to seismic behavior of structural systems. ACI Struct J 100:637–643

Carofilis W, Perrone D, O'Reilly GJ et al (2020) Seismic retrofit of existing school buildings in Italy: Performance evaluation and loss estimation. Eng Struct 225:111243. https://doi.org/10.1016/j.engstruct.2020.111243

Damcı E, Temur R, Bekdaş G, Sayin B (2015) Damages and causes on the structures during the October 23, 2011 Van earthquake in Turkey. Case Stud Constr Mater 3:112–131. https://doi.org/10.1016/j.cscm.2015.10.001

Deierlein G, Reinhorn A, Willford M (2010) NEHRP seismic design technical brief no. 4—nonlinear structural analysis for seismic design: a guide for practicing engineers. In: NIST

Demir S, Günaydin M, Atmaca B et al (2021) Performance evaluation of reinforced concrete buildings during the Sivrice-Elazığ earthquake (Mw = 6.8, January 24, 2020) in accordance with Turkish earthquake code. J Earthq Tsunami 15:2150018. https://doi.org/10.1142/S1793431121500184

Demirel IO, Yakut A, Binici B (2022) Seismic performance of mid-rise reinforced concrete buildings in Izmir Bayrakli after the 2020 Samos earthquake. Eng Fail Anal 137:106277. https://doi.org/10.1016/j.engfailanal.2022.106277

Di Ludovico M, Digrisolo A, Moroni C et al (2019) Remarks on damage and response of school buildings after the Central Italy earthquake sequence. Bull Earthq Eng. https://doi.org/10.1007/s10518-018-0332-x

Dogan G, Ecemis AS, Korkmaz SZ et al (2021) Buildings Damages after Elazığ, Turkey Earthquake on January 24, 2020. Nat Hazards 109:161–200. https://doi.org/10.1007/s11069-021-04831-5

Dumaru R, Rodrigues H, Varum H (2019) Cost-benefit analysis of retrofitted non-engineered and engineered buildings in Nepal using probabilistic approach. Soil Dyn Earthq Eng 122:1–15. https://doi.org/10.1016/j.soildyn.2019.04.004

Elnashai AS, Pinho R (1998) Repair and retrofitting of RC walls using selective techniques. J Earthq Eng 2:525–568

El-Sokkary H (2023) Nonlinear behaviour of FRP-retrofitted RC coupled shear walls. Structures 47:324–337. https://doi.org/10.1016/j.istruc.2022.10.142

Erange YGP, Jenothan M, Jayasinghe J, a. SC, et al (2023) Enhancement of the Lateral Performance of RC Columns Using Steel Jacketing: A Numerical Approach. Eng J Inst Eng Sri Lanka 56:51–64. https://doi.org/10.4038/engineer.v56i2.7576

Erdem I, Akyuz U, Ersoy U, Ozcebe G (2006) An experimental study on two different strengthening techniques for RC frames. Eng Struct 28:1843–1851. https://doi.org/10.1016/j.engstruct.2006.03.010

Gunes O (2015) Turkey's grand challenge: Disaster-proof building inventory within 20 years. Case Stud Constr Mater 2:18–34. https://doi.org/10.1016/j.cscm.2014.12.003

Haghpanah F, Foroughi H, Behrou R (2017) Sustainable seismic retrofitting of a RC building using performance based design approach. Eng Struct Technol 9:133–141. https://doi.org/10.3846/2029882X.2017.1380539

Hung C-C, Hsiao H-J, Shao Y, Yen C-H (2023) A comparative study on the seismic performance of RC beam-column joints retrofitted by ECC, FRP, and concrete jacketing methods. J Build Eng 64:105691. https://doi.org/10.1016/j.jobe.2022.105691

Jirsa JO, Kreger ME (1989) Recent research on repair and strengthening of reinforced concrete structures. In: ASCE, pp 679–688

Kucukgoncu H, Altun F (2020) The seismic behaviour of RC exterior shear walls used for strengthening of intact and damaged frames. Bull Earthq Eng 18:3683–3709. https://doi.org/10.1007/s10518-020-00839-7

Mander JB, Priestley MJN, Park R (1988) Theoretical stress-strain model for confined concrete. J Struct Eng 114:1804–1826. https://doi.org/10.1061/(ASCE)0733-9445(1988)114:8(1804)

Markou G (2021) A new method of seismic retrofitting cost analysis and effectiveness for reinforced concrete structures. Eng Struct 246:113083. https://doi.org/10.1016/j.engstruct.2021.113083

Martinelli A, Cifani G, Cialone G et al (2008) Building vulnerability assessment and damage scenarios in Celano (Italy) using a quick survey data-based methodology. Soil Dyn Earthq Eng 28:875–889. https://doi.org/10.1016/j.soildyn.2008.03.002

Meglio E, Longobardi G, Formisano A (2023) Integrated seismic-energy retrofit systems for preventing failure of a historical RC school building: comparison among metal lightweight exoskeleton solutions. Eng Fail Anal 154:107663. https://doi.org/10.1016/j.engfailanal.2023.107663

Menoni S (2001) Chains of damages and failures in a metropolitan environment: some observations on the Kobe earthquake in 1995. J Hazard Mater 86:101–119. https://doi.org/10.1016/S0304-3894(01)00257-6

Mertol HC, Tunç G, Akış T et al (2023) Investigation of RC Buildings after 6 February 2023, Kahramanmaraş, Türkiye Earthquakes. Buildings 13:1789. https://doi.org/10.3390/buildings13071789

Miura H, Midorikawa S, Fujimoto K et al (2008) Earthquake damage estimation in Metro Manila, Philippines based on seismic performance of buildings evaluated by local experts' judgments. Soil Dyn Earthq Eng 28:764–777. https://doi.org/10.1016/j.soildyn.2007.10.011

Oyguc R (2016) Seismic performance of RC school buildings after 2011 Van earthquakes. Bull Earthq Eng 14:821–847. https://doi.org/10.1007/s10518-015-9857-4

Pall A (2004) Performance-based design using pall friction dampers—an economical design solution. In: 13th world conference on earthquake engineering, Vancouver, BC, Canada, vol 71

Rizwan M, Ahmad N, Khan A (2019) Seismic performance of RC frame having low strength concrete: experimental and numerical studies. Earthq Struct 17:75–89. https://doi.org/10.12989/eas.2019.17.1.075

Rodrigues H, Furtado A, Vila-Pouca N et al (2018) Seismic Assessment of a School Building in Nepal and Analysis of Retrofitting Solutions. Int J Civ Eng 16:1573–1589. https://doi.org/10.1007/s40999-018-0297-9

Samadian D, Ghafory-Ashtiany M, Naderpour H, Eghbali M (2019) Seismic resilience evaluation based on vulnerability curves for existing and retrofitted typical RC school buildings. Soil Dyn Earthq Eng 127:105844. https://doi.org/10.1016/j.soildyn.2019.105844

Santos AF, Santiago A, Rizzano G (2019) Experimental response of friction dampers under different loading rates. Int J Impact Eng. https://doi.org/10.1016/j.ijimpeng.2019.103316

Sezen H, Whittaker AS, Elwood KJ, Mosalam KM (2003) Performance of reinforced concrete buildings during the August 17, 1999 Kocaeli, Turkey earthquake, and seismic design and construction practise in Turkey. Eng Struct 25:103–114. https://doi.org/10.1016/S0141-0296(02)00121-9

Sharma K, Deng L, Noguez CC (2016) Field investigation on the performance of building structures during the April 25, 2015, Gorkha earthquake in Nepal. Eng Struct 121:61–74. https://doi.org/10.1016/j.engstruct.2016.04.043

Sonuvar MO, Ozcebe G, Ersoy U (2004) Rehabilitation of reinforced concrete frames with reinforced concrete infills. ACI Struct J 101:494–500

Strategy and Budget Office (SBB) (2023). Post-earthquake assessment report. Retrieved from https://www.sbb.gov.tr/wp-content/uploads/2023/03/2023-Kahramanmaras-and-Hatay-EarthquakesReport.pdf

Souri O, Mofid M (2023) Seismic evaluation of concentrically braced steel frames equipped with yielding elements and BRBs. Res Eng 17:100853. https://doi.org/10.1016/j.rineng.2022.100853

Yakut A, Bakır BS, Yilmaz MT (2005) Re-examination of damage distribution in Adapazari: structural considerations. https://doi.org/10.1016/j.engstruct.2005.02.001

Turkish Building Earthquake Code-2018. Ankara, Türkiye

T.R. Ministry of Internal Affairs, Disaster and Emergency Management Presidency, Earthquake Department Turkey Acceleration Database and Analysis System, (AFAD-TADAS) https://tadas.afad.gov.en/ Accessed 11 Dec 2023

Publisher's Note Springer Nature remains neutral with regard to jurisdictional claims in published maps and institutional affiliations.